Journal of Membrane Science 545 (2018) 348–357

Contents lists available at ScienceDirect

Journal of Membrane Science

journal homepage: www.elsevier.com/locate/memsci

Chemical cleaning of ultrafiltration membranes for polymer-flooding wastewater treatment: Efficiency and molecular mechanisms

Guicai Liu[a,b], Lei Li[b], Liping Qiu[a], Shuili Yu[b,*], Ping Liu[d], Youbing Zhu[b], Jun Hu[c], Zhiyuan Liu[b], Dongsheng Zhao[b], Haijun Yang[c,*]

[a] School of Civil Engineering and Architecture, University of Jinan, Jinan 250022, PR China
[b] School of Environmental Science and Engineering, State Key Laboratory of Pollution Control and Resource Reuse, Tongji University, Shanghai, PR China, 200092
[c] Interfacial Water Division & Key Laboratory of Interfacial Physics and Technology, Shanghai Institute of Applied Physics, Chinese Academy of Sciences, PO Box 800-204, Shanghai 201800, PR China
[d] College of Architecture and Civil Engineering, Xi'an University of Science and Technology, Xi'an 710054, PR China

ARTICLE INFO

Keywords:
Polymer-flooding wastewater
Ultrafiltration membranes
Polymeric fouling
Chemical cleaning procedures
Pilot-scale experiments

ABSTRACT

In a polymer-flooding wastewater treatment process, physically irreversible fouling of ultrafiltration (UF) membranes is severe and inevitable. Particularly, anionic polyacrylamide (APAM) aggravated flux loss is a challenge in flux recovery. Chemical cleaning procedures for polyvinylidene fluoride (PVDF) UF membranes fouled by polymers (e.g., APAM) were designed by investigating their cleaning efficiency, synergistic effect and molecular interactions based on the molecular mechanisms of polymeric fouling. The cleaning efficiency and foulant–foulant intermolecular interactions indicated that the destruction of the hydrogen-bonded network, egg-box shaped gel network, and interpenetrating polymer network using sodium hypochlorite (NaClO), ethylenediaminetetraacetic acid (EDTA) and dodecyl trimethyl ammonium chloride (DTAC) solutions, respectively, led to significant flux recovery. The synergistic relationships between the two types of cleaning reagents were different in the mixed solutions and sequential procedures. In addition, oil emulsions facilitated the removal of APAM and slowed the flux loss. Finally, the flux recoveries and operational aspects in the pilot-scale UF experiments indicated that integration of the tested chemical cleaning procedures can efficiently remove membrane foulants and significantly restore membrane flux during polymer-flooding wastewater treatment of UF processes. These results are promising for controlling membrane fouling due to polymeric foulants.

1. Introduction

Anion polyacrylamide (APAM), a widely used polymeric additive [1,2], was used to enhance oil yield during the middle and later oilfield development periods in China. Consequently, a large amount of polymer-flooding wastewater (e.g., 3,000,000 m^3/d in the Daqing oilfields in China [3]) was produced during crude oil extraction, and this wastewater generally contained high concentrations of polymers (e.g., APAM) and salts [2–5]. Because of the potential risk to the environment, polymer-flooding wastewater must be treated prior to its reuse or discharge for economic and environmental benefits. The technologies for polymer-flooding wastewater treatment have been systematically summarized [5]. Among them, membrane separation processes, especially ultrafiltration (UF) processes, are extensively accepted for use [6] because of their advantages, which include the use of no chemical additives, low energy costs, and small space requirements. Our team developed a pilot-scale plan for a membrane process (consisting of UF, electrodialysis, and nanofiltration (NF) sections in sequence) to reuse polymer-flooding wastewater in the Daqing oilfields. However, physically irreversible fouling was severe and inevitable, even under the optimized operation conditions. APAM, which is abundant in polymer-flooding wastewater and is a major organic foulant, aggravated the flux loss [3,6,7] and made chemical cleaning of the fouled membranes challenging [3,8]. Therefore, the performance of chemical cleaning procedures for organic polymer foulants (e.g., APAM) plays a crucial role in the sustainable application of UF membranes.

To clean APAM during polymer-flooding wastewater treatment, the previously reported APAM characteristics and behaviors and mechanisms of the UF membrane fouling [3,7] should be considered when selecting the cleaning reagents and procedure. Carboxylates and amide groups make up the essential chemical segments of APAM molecules, and the APAM fouling layer is proposed to be a hydrogen-bonded network, an egg-box shaped gel network [3,9] and/or an interpenetrating polymer network [3]. Sodium hypochlorite (NaClO), which

* Corresponding authors.
E-mail addresses: ysl@tongji.edu.cn (S. Yu), yanghaijun@sinap.ac.cn (H. Yang).

http://dx.doi.org/10.1016/j.memsci.2017.08.062
Received 18 December 2016; Received in revised form 21 August 2017; Accepted 26 August 2017
Available online 30 August 2017
0376-7388/

can produce N–chlorination [8,10,11] and C–N hydrolysis [8,11] on amide groups, should be used to destroy the proposed hydrogen-bonded network and interpenetrating polymer network. Additionally, cationic surfactants (e.g., dodecyl trimethyl ammonium chloride (DTAC)), which can electrostatically bind to carboxylates (i.e., "strong polymer–surfactant interactions" [12,13]), should be introduced to promote the destruction of the interpenetrating polymer network. In addition, metal chelating reagents (e.g., ethylenediaminetetraacetic acid (EDTA)), which can bind the Ca^{2+} from the calcium–carboxylate complexes [14,15], should be used to disrupt the coordination bonds [3,16,17] between APAM and Ca^{2+} in the egg-box shaped gel network.

Acids, bases, metal chelating agents, surfactants, oxidants, and enzymes are usually applied in chemical cleaning to restore membrane performance [18–21]. NaClO is an available and cost-effective oxidant and has been used extensively to remove organic foulants [8,22] and to control biofouling [23–26]. However, NaClO is not particularly effective for removing hydrophilic, inorganic foulants [27] and metal-containing deposits [3,28]. Metal chelating agents, such as EDTA and sodium tripolyphosphate (STP), have been used to remove metal–organic complexes, but their cleaning efficiency varies with the feed solution. Simple cleaning with a caustic–EDTA solution can effectively remove humic [14] and alginic [15] foulants coordinated with Ca^{2+} and recover the membrane flux in pure water by disrupting the calcium–-carboxylate complexes in the gel layers. Formulated solutions containing metal chelating agents (e.g., EDTA and STP), anionic surfactants (e.g., sodium dodecyl sulfate (SDS)) and bases (e.g., sodium hydroxide (NaOH)), instead of simple caustic solutions of metal chelating agents, have been successfully used to clean metal–organic complexes from fouled membranes by biogas slurry concentration [29] and polymer-flooding wastewater [30] due to the synergistic effects of the cleaning reagents. The superior cleaning efficiency of the metal chelating agents for the humic/alginic substances was ascribed to the different molecular packing states of the gel layers. Anionic surfactants, such as SDS and sodium dodecyl benzene sulfonate (SDBS), can solubilize humic acid [14] and polymethyl acrylate (PMA) [31] because the hydrophobic portions of the surfactant molecules adsorb onto the foulant molecules through hydrophobic attraction [14]. In addition, when the surfactant concentration exceeds the critical micelle concentration (CMC), surfactant micelles begin to form in the cleaning solutions and provide more solubilization than the surfactant monomers [14]. In particular, SDS has a higher cleaning efficiency for lipids (more hydrophobic) than for polysaccharides and DNA [32]. Combinations of various agents can promote cleaning efficiency, simplify cleaning procedures, and decrease the cleaning frequency necessary for both formulated solutions and multiple-step procedures [21,29,30,33].

However, the majority of current reports focus on optimizing the dose, duration, and temperature of cleaning procedures [8,22,24–26,34–36], and examinations of the cleaning mechanisms are seldom involved. Hydrophobic and electrostatic attractions, which are the two basic interactions between surfactants and organic molecules, are considered weak and strong surfactant–organic interactions [12,13], respectively. In addition, the applications of strong surfactant–foulant interactions (i.e., electrostatic attractions between complementary groups of the surfactant and organic molecules) for cleaning organic foulants are highly limited. The cleaning efficiency of metal chelating agents was helpful for understanding molecular packing properties in varied gel layers and should attract more attention. Moreover, the distinct synergistic effects of various cleaning agents in multiple-step procedures and mixed solutions have rarely been reported. Additionally, crude oil, an incidental organic foulant, coexists with APAM in the fouling layer during the actual polymer-flooding wastewater UF treatment [3,7,8], and the roles of the crude oil in APAM fouling and cleaning should be investigated.

In this study, NaClO, EDTA, and surfactants, including cationic surfactants (e.g., DTAC), zwitterionic surfactants (e.g., dodecyl dimethyl betaine (BS-12)) and anionic surfactants (e.g., SDBS), were selected to remove APAM that was deposited onto polyvinylidene fluoride (PVDF) UF membranes. The cleaning efficiency and synergistic effects of the selected reagents were evaluated in terms of the membrane flux with pure water. In addition, the molecular mechanisms of APAM cleaning were investigated by analyzing atomic force microscopy (AFM) force curves. Additionally, the membrane fouling and cleaning when APAM and crude oil both are present were discussed. Ultimately, the optimized cleaning procedures were applied to pilot-scale UF experiments for polymer-flooding wastewater treatment, and a significant flux recovery performance was observed.

2. Materials and methods

2.1. Pilot-scale UF setup

A pilot-scale plant was built to treat and reuse polymer-flooding wastewater in the Daqing oilfield in China, and the plant consisted of sequential pretreatment, ultrafiltration (UF), electrodialysis, and nanofiltration (NF) processes (See Supplementary data, Fig. S1). The permeation of the UF setup met the requirements for oilfield injection or drainage [37], and the quality indexes are shown in Table S1.

The UF setup (with a treating capacity of 9800 t per day) is shown in Fig. 1 and has been running for more than 4 years. PVDF tubular composite UF membranes with hydrophilic modification were used. Approximate 700 membrane tubes formed one module with a total effective membrane area of 33.0 m^2. Two modules acted as one integrated unit, and seven units formed one processing section. The setup had two sequential sections. The first section treated the virgin feed solution, and the second section treated the concentrated solution from the first section. The permeation from both UF sections acted as the oilfield injection or drainage and the feed water for the electrodialysis setup.

Fig. 1. Images of the pilot-scale UF set-up (with a treatment capacity of 9800 t per day).

2.2. Materials and chemicals

Flat-sheet PVDF UF membranes with a mean pore size of 50 nm that were fabricated at the Shanghai Institute of Applied Physics (SINAP, China) were used for the bench-scale fouling and cleaning experiments. The outer surface and cross sectional images of the PVDF membrane are shown in Fig. S2, and the thickness, charge and contact angle are presented in Table S2. Hydrophilic groups, such as HO–/–COO^- and NH_2–/–NH–, were immobilized on the PVDF membrane surface [3]. The APAM was analytical grade, and its general structure, molecular weight and hydrolysis degree are presented in Fig. S3.

NaOH, HCl, NaClO, the sodium salt of EDTA, DTAC, BS-12 and SDBS were analytical grade and used as chemical cleaning reagents. The sodium chloride (NaCl) and calcium chloride ($CaCl_2$) used in all the experiments were analytical grade. Milli-Q purified water (18.2 MΩ cm) was used in all the experiments. The general structures of EDTA, DTAC, BS-12, and SDBS are presented in Fig. S4, and the CMC values of DTAC, BS-12, and SDBS are 19.0–21.7 [38–40], 1.39 [41], and 1.20–1.51 [42,43] mM, respectively.

2.3. Chemical cleaning procedures

At the end of the filtration, physical cleaning was implemented prior to the chemical cleaning. Three cleaning models, including simple cleaning with a single reagent, multiple-step cleaning with two types of reagents, and one-step cleaning with formulated solutions containing two types of reagents, were used in both the pilot- and bench-scale experiments.

For the pilot-scale experiments, physical and chemical cleanings were implemented in situ. At the end of the filtration, the fouled membranes were rinsed with NF permeation water for 30 min, and the rinse water was discharged. Then, the fouled membranes were backwashed with NF permeation water for 30 min, and the backwashing water was discharged. Subsequently, the fouled membranes were soaked in a chemical cleaning solution for one hour, and then, they were backwashed for 30 min and rinsed for 30 min with NF permeation water. After the cleaning, the fouled membranes were soaked in NF permeation water until they were used for another filtration.

For the bench-scale experiments, the fouled membranes were detached from a dead-end filtration system [6] and rinsed with deionized (DI) water. The membrane was then installed in the filtration system and further rinsed with 200 mL of DI water at a stirring speed of 300 rpm for 15 min. Subsequently, this membrane was placed in a beaker containing 300 mL of the selected chemical reagent for 1 h at ambient temperature (adjusted to approximately 25 °C using an air-conditioner). Then, the membrane was rinsed with enough DI water to remove any residual chemical solution. Finally, the membranes were installed, and their flux with pure water was determined using a trans membrane pressure (TMP) of 0.05 MPa, which was the same pressure used in the fouling experiments. At least two replicates of the fouling and cleaning experiments were performed for each cleaning model. Other details of the bench-scale experiments were previously reported [3].

The selected chemical reagent solutions were NaClO, EDTA, DTAC, BS-12, and SDBS solutions at a pH of 12.0. The NaClO solution had a volume percent of 0.2%, and the molar concentrations of the DTAC, BS-12, and SDBS solutions were ~4.0 times their respective CMCs, 76, 5.56 and 4.80 mM, respectively. The molar concentration of EDTA was 10 mM. The concentrations and pH values of the single chemical cleaning solutions were identical to those of the formulated cleaning solutions.

The flux recovery of the fouled membrane after one cleaning step was defined as a percentage ratio of the flux restored (flux increment after and prior to the cleaning step) in the fouled membrane to the initial flux of the virgin membrane, as shown in Eqs. (1) and (2).

$$r_w = \frac{J_{wc} - J_{wc'}}{J_{w0}} \quad (1)$$

$$r_v = \frac{J_{vc} - J_{vc'}}{J_{v0}} \quad (2)$$

where r_w and r_v are the flux recoveries of the pure water flux and wastewater permeation flux, respectively; $J_{wc'}$ and J_{wc} are the pure water fluxes of the fouled membrane prior to and after one of the cleaning steps in the bench-scale experiments; $J_{vc'}$ and J_{vc} are the wastewater permeation fluxes of the fouled membrane prior to and after one of the cleaning steps in the pilot-scale experiments; and J_{w0} and J_{v0} are the initial pure water flux and permeation flux of the pristine membrane. In addition, the baselines for r_w and r_v are defined as Eqs. (3) and (4), respectively:

$$r_{wb} = \frac{J_{wf} - 0}{J_{w0}} \quad (3)$$

$$r_{vb} = \frac{J_{vf} - 0}{J_{v0}} \quad (4)$$

where J_{wf} and J_{vf} are the pure water flux and wastewater permeation flux of the fouled membrane for the bench- and pilot-scale experiments, respectively.

2.4. Analytical methods

Fourier transform infrared spectroscopy (FTIR) of APAM before and after soaking in NaClO were obtained using Nicolet 5700 (Nicolet, USA). A spectrum, collected as the average of 32 scans with a resolution of 4 cm^{-1}, was recorded from 4000 to 400 cm^{-1}. All spectra were collected with Omnic 8.0 software. Concentrations of eluotropic calcium were determined on an inductively coupled plasma emission spectrometer (ICP-Agilent 720E). Surface morphologies of the fouled membranes, in the case of APAM coexisted with and without crude oil, were examined by a scanning electron microscope (XL30FEG, Philips, Netherlands) subsequence to be dried by vacuum freeze drying and sputter-coated with a thin layer of gold for conductivity.

2.5. Intermolecular interaction measurements

A MultiMode 8 at. force microscope equipped with a NanoScope V controller (Bruker, Germany) was used to perform the interaction force measurements between the APAM-substrates and APAM-tips. The silicon (Si) substrates and the probe tips used in this paper were covalently modified with APAM molecules before use [3]. The force measurements were performed using a contact-mechanics mode [44,45] in 14.0 mM $CaCl_2$, 10 mM EDTA, 1.0 mM, 1.0 CMC equivalent, and 4.0 CMC equivalent DTAC solutions at 25 °C. Additionally, the contact probe (CSG11, NT-M DT, Russia) tips had a typical curvature radius of 10 nm, and the spring constants of their cantilevers were determined to be 0.298–0.310 N/m in our experiments. In all cases, over sixty force curves at different locations were acquired and analyzed with the Nanoscope Analysis 1.40 software.

3. Results and discussion

3.1. Flux recoveries

The cleaning efficiency and synergistic effects of the selected reagents for APAM removal were investigated (see Figs. 2 and 3), and the relations between the flux recoveries and eluotropic calcium (Ca^{2+}) concentrations are provided as well (see Fig. 4).

3.1.1. Comparison of the cleaning efficiency among simple reagents

The flux recoveries for simple cleaning with the cationic surfactants (e.g., DTAC), zwitterionic surfactants (e.g., BS-12), anionic surfactants

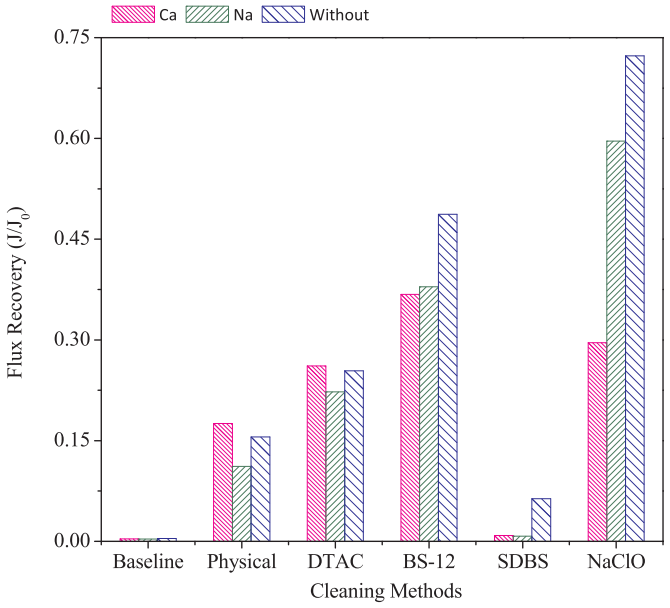

Fig. 2. Comparison of flux recoveries among simple cleaning reagents aqueous solutions at a pH of 12 in the bench-scale experiments. Sodium hypochlorite solution was at a volume percent of 0.2%, and the molar concentrations of DTAC, BS-12, and SDBS solutions were ~ 4.0 times of their respective critical micelle concentrations (CMC), with 76, 5.56 and 4.80 mM, respectively. Without: membranes fouled by APAM solutions without addition of salts; Na and Ca: membranes fouled by APAM solutions with addition of 40 mM NaCl and 14 mM $CaCl_2$.

(e.g., SDBS), and NaClO are presented in Fig. 2. The flux recoveries for all the tested simple reagents decreased in the following order, NaClO (0.72) > BS-12 (0.49) > DTAC (0.25) > SDBS (0.063), NaClO (0.60) > BS-12 (0.38) > DTAC (0.22) > SDBS (0.0077), and BS-12 (0.37) > NaClO (0.30) ≈ DTAC (0.26) > SDBS (0.0088) for the membranes fouled by APAM solutions without any salts ("without"), with 40 mM NaCl ("Na") and with 14.0 mM $CaCl_2$ ("Ca"), respectively. For the APAM cleaning, the cationic and zwitterionic surfactants and NaClO resulted in significant flux recoveries, but the anionic surfactants provided almost no cleaning effect. These results are consistent with the cleaning mechanisms that were discussed in detail when presenting the foulant–foulant interactions in the cleaning reagent solutions.

The decreasing order of the flux recoveries for the "without" samples was the same as that for "Na" but different from that for "Ca", as shown in Fig. 2. For NaClO, the flux recoveries decreased as "without" (0.72) > "Na" (0.60) > "Ca" (0.30), which indicated that addition of salts, particularly Ca^{2+}, created challenges for the APAM cleaning with NaClO. However, with the cationic surfactants (e.g., DTAC), the flux recoveries decreased in the following order, "without" (0.25) ≈ "Na" (0.22) ≈ "Ca" (0.26), which indicated that the salts had a negligible impact on the APAM cleaning with cationic surfactants. For the zwitterionic surfactants (e.g., BS-12), the flux recoveries decreased in the following order, "without" (0.49) > "Na" (0.38) ≈ "Ca" (0.37), and no difference was observed between the "Na" and "Ca" samples even though both have a minor impact on the cleaning efficiency. The differences in the order of the flux recoveries among NaClO and the surfactants (e.g., DTAC and BS-12) were ascribed to the distinct APAM cleaning mechanisms. In particular, upon the addition of 14 mM Ca^{2+}, the total flux recoveries for all the tested reagents only changed from 0.42 (= 0.16 + 0.26) to 0.54 (= 0.16 + 0.38), which indicated that Ca made the APAM cleaning difficult. Further investigations on chemical cleaning for APAM–Ca complexes are discussed later.

3.1.2. *Synergistic effects of varied reagents for multiple-step procedures and formulated solutions*

To obtain a greater cleaning efficiency, two different reagents were used in the multiple-step procedures and formulated solutions, and the flux recoveries after the removal of the APAM–Ca complex using these two collaborative models are shown in Fig. 3(a) and (b), respectively. Simultaneously, the synergistic relationships between the two different reagents in the two collaborative models (the multiple-step procedures and the formulated solutions) were investigated to further understand the APAM fouling and cleaning mechanisms. Moreover, EDTA was used

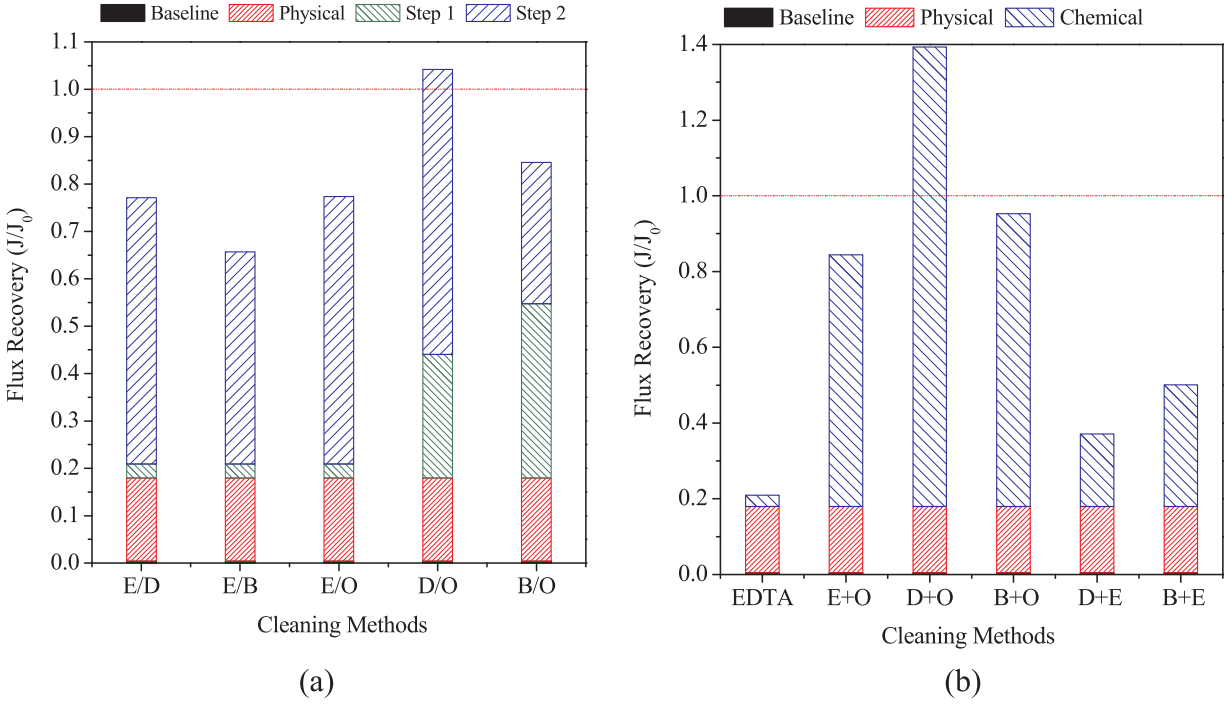

Fig. 3. Flux recoveries for (a) multiple-step procedures, and (b) formulated solutions in the bench-scale experiments. "/" and "+" represent cleanings with multiple-step procedures and formulated solutions, respectively. "E", "D", "B", and "O" represent EDTA, DATC, BS-12 and NaClO solutions, respectively, which had same concentrations to both the two collaborative models. Herein, the concentrations of EDTA, DATC, BS-12 and NaClO solutions were 10 mM, 76 mM, 5.56 mM and 0.2% (volume percent), respectively.

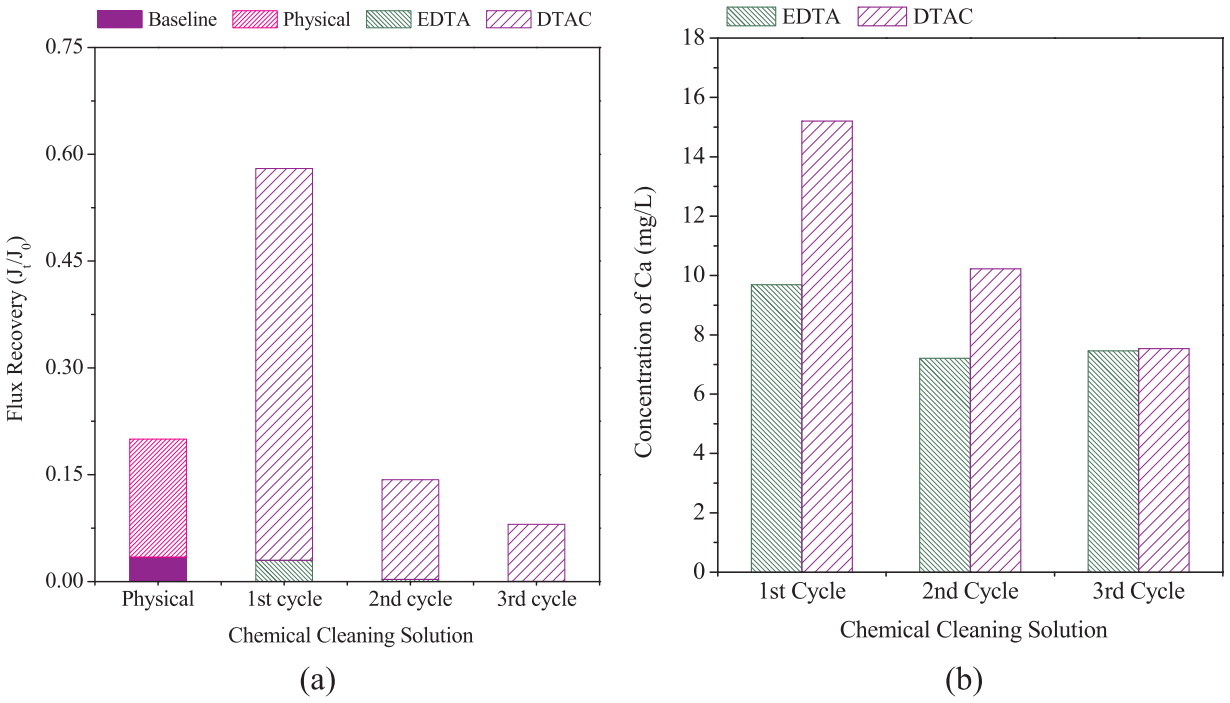

Fig. 4. For EDTA/DTAC cleaning procedure in the bench-scale experiments, (a): flux recoveries, and (b): eluotropic Ca^{2+} concentration. The multiple-step cleaning procedure of EDTA/DTAC was continuously repeated three times for one fouled membranes, and its each implement was named the 1st E/D, 2nd E/D and 3rd E/D in sequential. Herein, the concentrations of EDTA and DATC were 10 and 76 mM, respectively.

to disrupt the APAM–Ca complexes based on the specific role of Ca in the APAM fouling [3].

The flux recoveries after the removal of the APAM–Ca complex via multiple-step alternative cleanings with two types of reagent are presented in Fig. 3(a). For the E/D, E/B, and E/O cleaning procedures, the flux recovery after the first cleaning step with EDTA was merely 0.03, which was likely due to the existence of the interpenetrating polymer network [3], except for the egg-box shaped gel network, in the APAM–Ca gel layer. Following the second cleaning step with DTAC, BS-12, and NaClO, the flux recoveries were 0.56, 0.45, and 0.56, respectively, which were all higher than those for the corresponding simple cleaning and indicated that the first cleaning step with EDTA significantly enhanced the cleaning effectiveness of the second steps. With D/O, the flux recovery was 0.26 for the first step with DTAC, and the recovery for the second step with NaClO was 0.60, which was higher than that for the simple cleaning with NaClO (0.30) and indicated that the first cleaning step with DTAC could enhance the cleaning effectiveness of the second step with NaClO. In contrast, with B/O, the flux recovery for the first step with BS-12 was 0.37, and the recovery for the second step with NaClO was 0.30, which was the same as that for the simple cleaning with NaClO and indicated an insignificant synergistic relationship between BS-12 and NaClO for cleaning APAM–Ca in a two-step procedure.

Formulated solutions containing two types of reagents were used to further investigate the synergistic relationships among the varied reagents, and the corresponding flux recoveries are presented in Fig. 3(b). The flux recoveries were 0.66, 0.77, and 1.21, respectively, for the formulated solutions of NaClO with EDTA, BS-12, and DTAC (E + O, B + O and D + O, respectively), and the values were all higher than those obtained with the simple cleaning. In particular, the formulated solution of NaClO and DTAC (D + O) provided a total flux recovery of 1.39, which increased by 39% as compared with the permeation flux with ultrapure water of a virgin membrane, and this results was most likely due to the hydrophilic modification of the membrane surfaces caused by the combination of DTAC and NaClO at pH = 12.0 [46,47]. The hydrophilic modification was further verified by the flux recoveries exceeding that of the original membranes (see Fig. S5).

The synergistic relationships between the two types of reagents in the multiple-step cleaning procedures were different from those of the formulated solutions. With the formulated solution of EDTA and DTAC, the flux recovery was 0.19 (see Fig. 3(b)), which was lower than that of the simple cleaning and the two-step procedures. This result indicated an inhibiting relationship. The inhibition interactions between EDTA and DTAC distinct from the significant synergistic relationship for the sequential E/D procedures are highly possible due to the formation of weak electrolytes (with larger molecular dimensions) via the electrostatic attractions among the EDTA carboxylates and the positively charged DTAC groups in the mixed solutions. In contrast, the flux recovery for D + O was 1.21 (see Fig. 3(b)), which was higher than that for D/O (0.86 = 0.26 + 0.60) (see Fig. 3(a)) and showed the more prominent synergistic effects for the mixed cleaning solution of DTAC and NaClO. This indicated that the formulated solutions with two synergistic reagents could provide more noticeable hydrophilic modifications on the membrane surfaces (caused by the combination of DTAC and NaClO) than the step-based process. The results for E + B and E/B were similar to those for E + D and E/D. Additionally, the flux recovery for E + O was 0.66, which was slightly higher than the recovery, 0.59 (= 0.03 + 0.56), for E/O (see Fig. 3(a) and (b)), which indicated a minor difference in the cleaning efficiency for the two collaborative models, negligible interactions between EDTA and NaClO and minimal hydrophilic modifications on the membrane surfaces.

3.1.3. Relationships between the flux recoveries and eluotropic Ca^{2+} concentrations

To further understand the destruction of the APAM–Ca complexes, the relationships between the E/D flux recoveries and the corresponding eluotropic Ca^{2+} concentrations were discussed via a contrastive analysis of Fig. 4(a) and (b). With the first EDTA step in the E/D mode, the flux recoveries for the three repetitions of 1–EDTA, 2–EDTA, and 3–EDTA were 0.03, 0.0029 and 0.0004 (see Fig. 4(a)), respectively, and the corresponding eluotropic Ca^{2+} concentrations (mg/L) were 9.69, 7.21, and 7.46 (see Fig. 4(b)), respectively. The notable Ca^{2+}

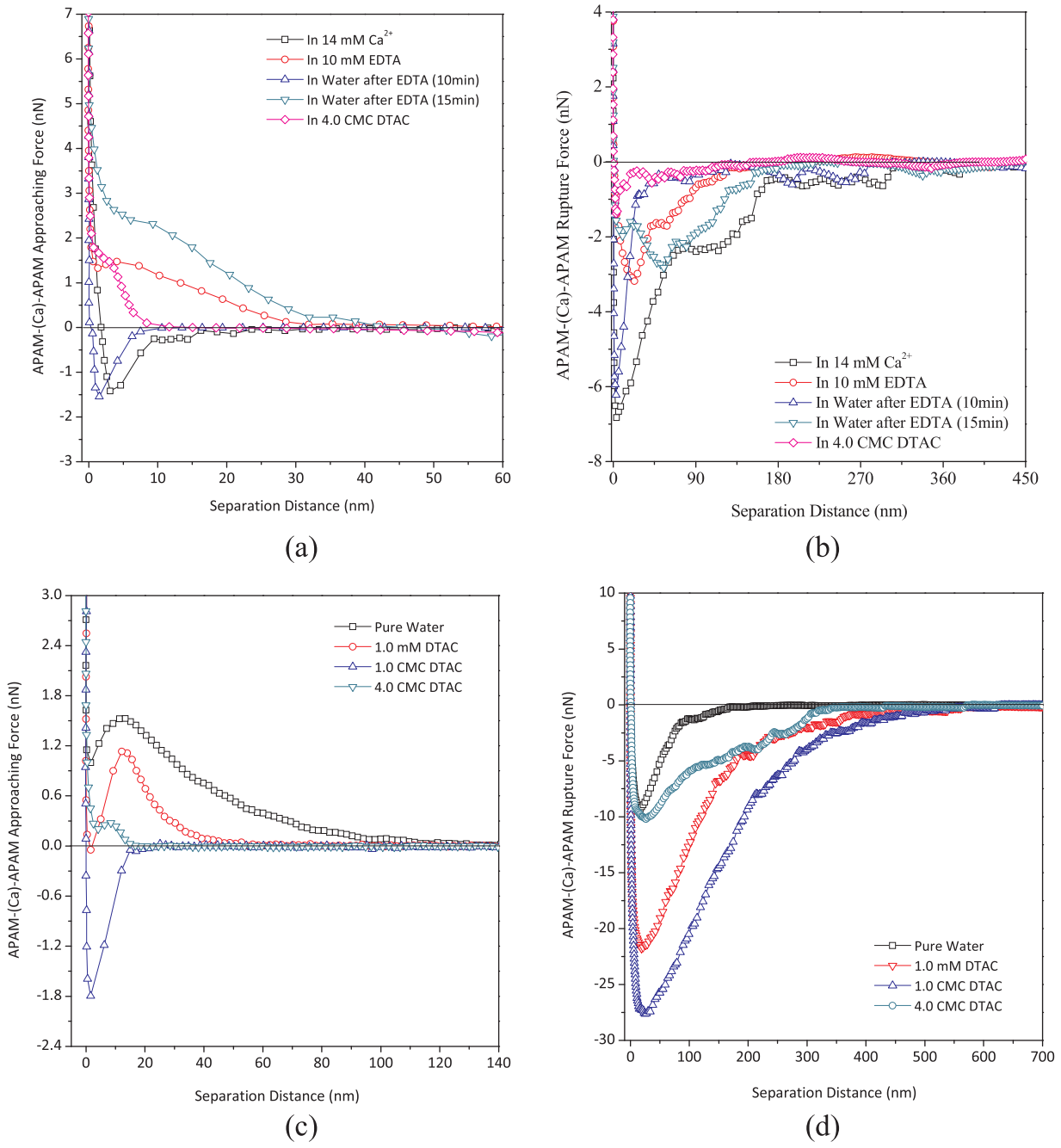

Fig. 5. APAM-(Ca)-APAM intermolecular interactions in the EDTA solutions and DTAC solutions. (a) and (b): approaching force curves and rupture force curves in the EDTA solutions, respectively; (c) and (d): approaching force curves and rupture force curves in the DTAC solutions, respectively. For (a) and (b): First, APAM-APAM forces were measured in 14.0 mM $CaCl_2$ and 10 mM EDTA solution, sequently; then, after the tip and substrate being soaked in the 10 mM EDTA solution for 10 min and 15 min, respectively, the two force curves were measured in pure water; finally, the force curves were obtained in 4.0 CMC DTAC. For (c) and (d): these force curves were measured in pure water, 1 mM, 1CMC and 4.0 CMC DTAC solutions, sequently. In addition, the tip and substrate were rinsed with pure water after each measurement.

concentrations in the eluents confirmed that EDTA removed Ca from the APAM–Ca complexes, which agreed with the results shown in Fig. 5(a) and (b). In conjunction with the minor flux recovery for EDTA, these results confirmed the structural heterogeneity of the integral APAM–Ca gel layer (as discussed in Fig. 3).

With the second DTAC step in the E/D mode, the flux recoveries for the three repetitions of 1–DTAC, 2–DTAC, and 3–DTAC were 0.55, 0.14, and 0.08 (see Fig. 4(a)), respectively, and the corresponding eluotropic Ca^{2+} concentrations (mg/L) were 15.21, 10.22, and 7.53 (see in Fig. 4(b)), respectively. The decreasing order of the flux recoveries for the second cleaning step with DTAC was identical to that of the corresponding eluotropic Ca^{2+} concentrations, and this was most likely due to DTAC–APAM interactions, which can neutralize the sum adhesion energies of the APAM–Ca coordination bonds and the APAM–APAM intermolecular entanglements to promote the destruction of the entire APAM–Ca gel layer and a significant flux recovery. In the E/D mode, continuously repeating the cleaning with the same reagents did not result in any flux recovery, but circular, alternating permutations of EDTA and DTAC achieved a notable flux recovery. Moreover, even though EDTA had only a slight cleaning effect, it enhanced the flux recovery after the DTAC cleaning. Accordingly, prior cleaning with EDTA played a crucial role in the removal of the APAM–Ca complexes.

Overall, the flux recoveries after chemical cleaning showed that the cationic surfactants (e.g., DTAC) and zwitterionic surfactants (e.g., BS-

12), rather than the anionic surfactants (e.g., SDBS), were effective for the APAM cleaning along with NaClO. For the APAM–Ca cleaning, EDTA was introduced, and its minor flux recovery and the significant eluotropic Ca^{2+} concentration indicated that the interpenetrating polymer network co-existed with the egg-box shaped gel network in an integral APAM–Ca gel layer. The synergistic relationships between the two types of cleaning reagents were different from those of the formulated solutions and the multiple-step procedures. The interactions between the cleaning reagents and APAM molecules require further investigation.

3.2. Foulant–foulant molecular interactions during chemical cleaning

Based on the flux recoveries for the tested cleaning procedures and the previously reported APAM fouling molecular mechanisms [3], the molecular interactions between APAM and the tested, effective reagents, including NaClO, EDTA and DTAC, are presented below.

FTIR spectra of APAM before and after reacting with NaClO indicated that NaClO caused N–chlorination and C–N hydrolysis [11] in the APAM amide groups, as shown in Fig. S6. The polymerization of the intermolecular-hydrogen bonds (between $-C^{=}O/^{-}OOC-$ and $-N-H/-C-H$) and the intermolecular entanglements among the APAM chains were likely destroyed following the disintegration of the APAM amides and the generation of APAM carboxylates ($^{-}OOC-$) by C–N hydrolysis. Consequently, the hydrogen-bonded network and the interpenetrating polymer network were likely destroyed by NaClO, which resulted in the significant flux recovery (see Figs. 2 and 3). Moreover, the APAM–(Ca)–APAM intermolecular interactions in the EDTA and DTAC solutions were investigated to reveal the molecular mechanisms of APAM cleaning by EDTA and DTAC, and the results are presented in Fig. 5.

3.2.1. Roles of EDTA in the APAM–(Ca)–APAM intermolecular interactions

The APAM–(Ca)–APAM approaching intermolecular force was attractive (–1.42 nN at 3.10 nm) in a 14 mM $CaCl_2$ solution, as shown in Fig. 5(a). However, the attractive force became a repulsive force of +2.0 nN (with an interaction distance of 28.0 nm) in a 10 mM EDTA solution. The explanation for this was that the free EDTA removed Ca^{2+} from the APAM–Ca complexes and released the free carboxylates ($–COO^{-}$) of the APAM molecules (covalently bound onto the tip and substrate) by forming a more stable EDTA–Ca complex, which resulted in enhanced electrostatic repulsions among the APAM carboxylates ($–COO^{-}$). This repulsion was consistent with the significant Ca^{2+} concentrations in the EDTA eluent (see Fig. 4(b)). After the tip and substrate were soaked in the EDTA solution for 10 min, the approaching force in pure water was attractive (−1.54 nN at 1.51 nm), which indicated the existence of residual Ca^{2+} in the APAM–Ca complexes. Upon increasing the soaking time to 15 min, the approaching force became repulsive (+4.0 nN with an interaction distance of 38.6 nm), which indicated a kinetic component of the competition. The minimum reaction time for EDTA to destroy the monomolecular layer of the APAM–Ca complexes was 15 min, which should be the baseline cleaning duration for the APAM–Ca removal by EDTA.

A similar phenomena also appeared in the APAM–(Ca)–APAM rupture force curves acquired in EDTA solutions. For example, the maximum adhesion force ($F_{ad,max}$) of APAM–(Ca)–APAM was −6.82 nN in a $CaCl_2$ solution, and the $F_{ad,max}$ was reduced to −3.18 nN in an EDTA solution, as presented in Fig. 5(b). This change was attributed to an enhancement in the electrostatic repulsion among the APAM carboxylates, which is shown in Fig. 5(a). The $F_{ad,max}$ values also showed a kinetic dependence, which can be attributed to the reason mentioned above.

3.2.2. Roles of DTAC in APAM–APAM intermolecular interactions

The APAM–(Ca)–APAM $F_{ad,max}$ value was the smallest (−1.38 nN at 3.24 nm) with the shortest interaction distance of 114.86 nm in a 4.0 CMC equivalent DTAC solution (after first soaking in the EDTA solution for 15 min, see Fig. 5(b)), which indicated that DTAC could significantly reduce both the values and interaction distance of the foulant–foulant adhesion force. For the same reason, the approaching force of APAM–(Ca)–APAM in the DTAC solution was repulsive (+2.10 nN with an interaction distance of 6.46 nm, see Fig. 5(a)), which kept the foulant molecules from redeposition when the foulant concentration did not exceed the dilute/semidilute threshold, C* (When the foulant concentration exceeded C*, the polymeric chains began to overlap.) [48,49]. To distinguish the roles of the DTAC monomers and micelles in the APAM cleaning, the APAM–APAM interactions in DTAC solutions with various concentrations were further investigated (see Fig. 5(c) and (d)).

The APAM–APAM approaching force curves varied with the DTAC concentrations, as presented in Fig. 5(c). The repulsive approaching forces decreased from +1.0 ~ +2.0 nN (in pure water) to 0 ~ +1.0 nN upon the addition of 1 mM of DTAC. With addition of 1 CMC equivalent of DTAC, the repulsive approaching force became an attractive force with a maximum value of −1.8 nN. However, further increasing the DTAC concentration to 4.0 CMC equivalents caused the attractive approaching force to become a repulsive force (+0.45 nN). The attractive approaching forces for a 1.0 CMC equivalent DTAC solution were derived from the hydrophobic interactions [50,51] among the external hydrophobic ends of the DTAC monomers, which were bound to the APAM chains (see Fig. S7). For the same reason, the approaching repulsion decreased in a 1 mM DTAC solution. In contrast, the repulsive approaching forces for a 4.0 CMC equivalent DTAC solution were caused by the electrostatic repulsions among the DTAC micelles bound to the carbon skeleton and carboxylates ($–COO^{-}$) of the APAM. Accordingly, the DTAC monomers clearly displayed a dominant role in the APAM–DTAC interactions in the 1 CMC equivalent DTAC solution and generated APAM–(DTAC monomer) complexes (see Fig. S7). Alternatively, the DTAC micelles dominated the APAM–DTAC intermolecular interactions in the 4.0 CMC equivalent DTAC solution and produced APAM–(DTAC micelle) complexes, which were created by the hydrophobic interactions among the DTAC monomers and APAM–(DTAC monomers) and/or the electrostatic attractions among the DTAC micelles and APAM COO^{-} groups (see Fig. S7).

As shown in Fig. 5(d), the APAM–APAM $F_{ad,max}$ was attractive (−9.33 nN at 14.66 nm) in pure water, increased to −21.78 nN (at 19.11 nm) and −27.64 nN (at 24.96 nm), and then decreased to −10.20 nN (at 26.94 nm) upon the sequential addition of 1.0 mM, 1.0 CMC and 4.0 CMC equivalent DTAC aqueous solutions. The increase in the $F_{ad,max}$ values was due to the aforementioned hydrophobic interactions among the DTAC monomers, and the reduction in the $F_{ad,max}$ value was attributed to the electrostatic repulsions among the DTAC micelles. Combining the approaching and rupture force curves showed that the DTAC micelles, not the monomers, enhanced the APAM–APAM repulsions, which facilitated the destruction of the interpenetrating polymer network and cleaned the APAM [52]. This result is consistent with the significant flux recovery for the 4.0 CMC equivalent DTAC solutions, as presented in Figs. 2–5, 7 and 8.

In summary, combining the foulant–foulant intermolecular interactions and flux recoveries indicated that the destruction of the hydrogen-bonded network, the egg-box shaped gel network, and the interpenetrating polymer network using NaClO, EDTA and DTAC solutions led to significant flux recoveries. NaClO caused N–chlorination and C–N hydrolysis of the APAM amide groups to destroy the hydrogen-bonded and interpenetrating polymer networks in the APAM fouling layer. For the EDTA solutions, the APAM–(Ca)–APAM intermolecular interactions indicated a complete disruption of a monomolecular layer of the APAM–Ca complexes with a minimum reaction time of 15 min. For the DTAC solutions, the APAM–APAM interactions showed that the DTAC micelles, not the monomers, enhanced the APAM–APAM intermolecular repulsions and

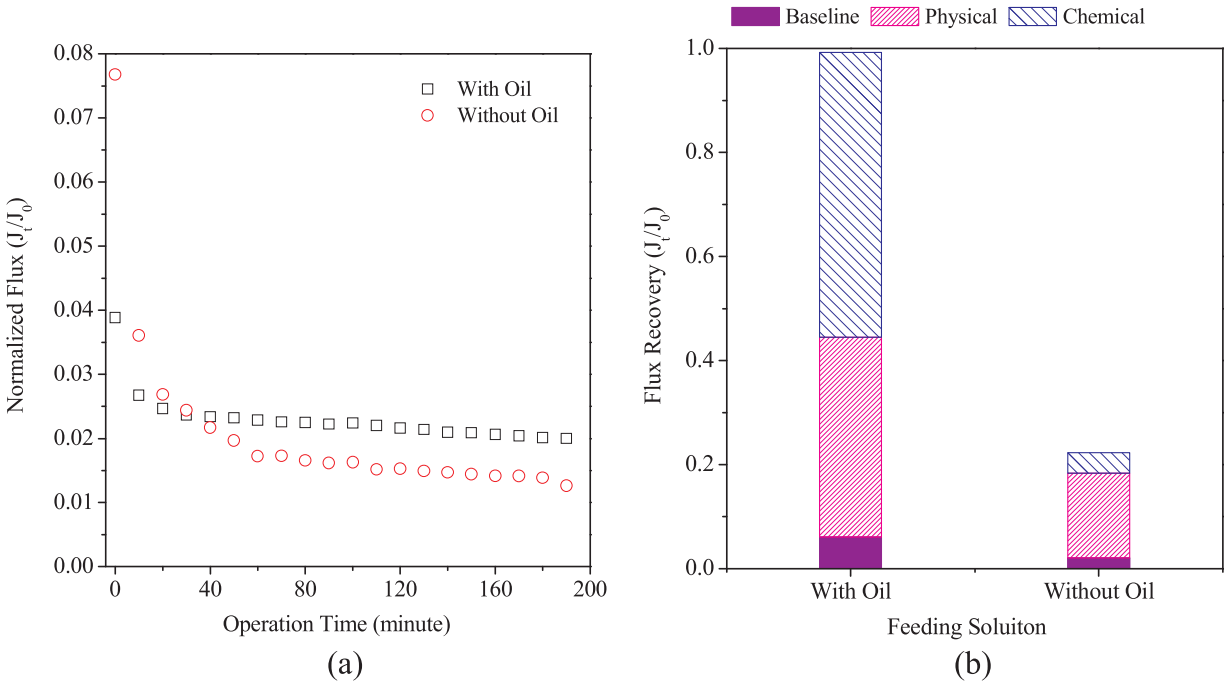

Fig. 6. Membrane (a) fouling and (b) cleaning for APAM co-existing with crude oil in the bench-scale experiments. Without oil: 400 mg/L APAM solution containing 1.4 mM $CaCl_2$ + 37.0 mM NaCl; With oil: actual polymer-flooding wastewater after filtration by 1.0 μm PVDF membrane, which containing 400 mg/L APAM, 22–37 mg/L crude oil, 1.4 mM $CaCl_2$, and 37.0 mM NaCl. For (a), J_0 is the permeation flux of virgin membranes with pure water and J_t is the membrane flux with the feeding solutions. For (b), the cleaning methods were the multiple-step way by using SDBS and EDTA, and were same for both the two cases. Herein, the concentrations of EDTA and SDBS solutions were 10 and 4.80 mM, respectively.

promoted the destruction of the interpenetrating polymer network. The membrane fouling and cleaning when APAM and crude oil are both present are further discussed below to understand their mechanisms in UF treatment for actual polymer-flooding wastewater.

3.3. Membrane cleaning for APAM and crude oil

Crude oil coexists with APAM in the actual polymer-flooding wastewater and in the fouling layers [3,7]. To simulate these practical situations, the membrane fouling and cleaning processes for APAM with crude oil are presented in Fig. 6, including the flux declines and recoveries.

The presence of crude oil significantly slowed the flux loss and facilitated the physical and chemical cleaning, as shown in Fig. 6. For crude oil with APAM ("with oil"), the flux loss was reduced in comparison with that for the feeding solution without the addition of crude oil ("without oil") (see Fig. 6(a)). Correspondingly, the flux recoveries for "with oil" after the physical and chemical cleaning were 0.3848 and 0.5474, respectively, which were higher than the recoveries of 0.1629 and 0.0394 for "without oil" (see Fig. 6(b)). In conjunction with the SEM morphologies of the fouled membranes (see Fig. S8), a reasonable explanation for these results was that the oil emulsions provided a steric hindrance that impeded the interactions of both the APAM–membrane and APAM–(Ca)–APAM and resulted in a fragmentary structure of the polymeric network in the "with oil" sample. The proposed fragmentary polymeric network was not compact and could be facilely cleaned in comparison with that of the intact structure for the "without oil" sample.

3.4. Applications in pilot-scale experiments

To evaluate the practicality of the procedures, the chemical cleaning procedures discussed above were used in the pilot-scale UF setup (see Fig. 1) to treat polymer-flooding wastewater. The flux recoveries and operational aspects are presented in Figs. 7 and 8, respectively.

The flux recoveries for the tested cleaning procedures in the pilot-scale UF experiments are shown in Fig. 7. After a simple EDTA cleaning, the fouled membranes that were used with the polymer-flooding wastewater had a significant flux recovery of 0.34. This was attributed to the co-existing crude oil (see Section 3.3). Upon the addition of NaClO to the EDTA cleaning solution (E + O), the flux recovery decreased to 0.30, which was ascribed to NaClO enhancing the attraction of the petroleum hydrocarbon for the PVDF membrane surface [47,53].

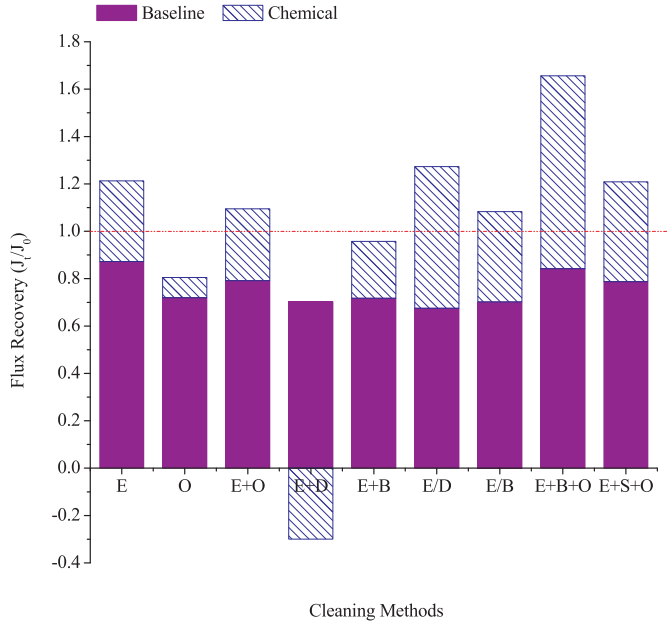

Fig. 7. Flux recoveries for the cleaning methods in the pilot-scale experiments. "/" and "+" represent cleanings with sequential procedures and formulated solutions, respectively. "E", "D", "B", "S", and "O" represent EDTA, DATC, BS-12, SDBS, and NaClO solutions, respectively, the concentrations of which were 10, 76, 5.56, 4.80 mM and 0.2%(volume percent), respectively.

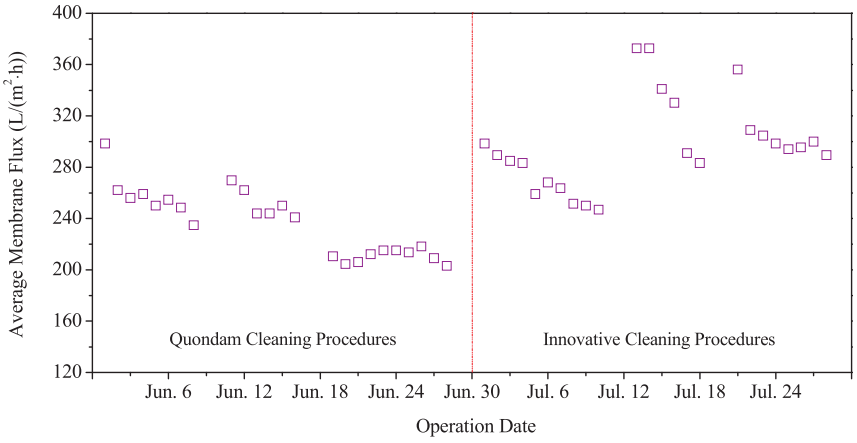

Fig. 8. Comparison of operational aspects between the quondam and innovative cleaning procedures for one unit of the pilot-scale UF set-up. The quondam and innovative cleaning procedures represented the commercial cleaning methods and the integration of the efficient cleaning methods discussed above, respectively. The quondam cleaning procedures were used until Jul. 1, 2105, from then on, the innovative cleaning procedures started to be used. Herein, operation status of the tested UF unit for the quondam and innovative cleaning procedures corresponded to one month before and after Jul. 1, 2105, respectively, both of which contained three sequent cycles of filtration. For the quondam cleaning procedures, the first, second and third cycle of filtration corresponded to Jun. 1 ~ Jun. 8, Jun. 11 ~ Jun. 16 and Jun. 19 ~ Jun. 28, respectively; and for the innovative cleaning procedures, the first, second and third cycle of filtration corresponded to Jun. 1 ~ Jun. 10, Jun. 13 ~ Jun. 18 and Jun. 21 ~ Jun. 28, respectively.

Similarly, when DTAC or BS-12 was added to the EDTA solution (E + D and E + B, respectively), the flux recoveries decreased to –0.30 and 0.24 (see Fig. 7), respectively, due to the inhibition interactions between the two different reagents (see Section 3.2). In contrast, by simultaneously adding NaClO and surfactants to the EDTA solutions (E + B + O), the flux recovery was significantly enhanced to 0.81 due to the hydrophilic modification of the PVDF membrane surface (see Section 3.2). Alternatively, when a sequential cleaning with surfactants after a single cleaning with EDTA (E/D and E/B) was implemented, the flux recovery significantly increased from 0.34 to 0.60 for E/D and slightly increased to 0.38 for E/B, which indicated that the cationic surfactant (DTAC) was more effective than the zwitterionic surfactant (BS-12) in the sequential process.

Compared to the results from quondam commercial cleaning procedures, these innovative cleaning procedures (e.g., the integration of the efficient cleaning methods discussed above) resulted in significantly higher flux recoveries and higher membrane fluxes with polymer-flooding wastewater, as presented in Fig. 8. For the quondam and innovative cleaning procedures, the initial fluxes (L/(m^2 h)) after chemical cleaning were 210.6–298.5 and 298.5–372.7, respectively, and the corresponding final fluxes (L/(m^2 h)) were 209.1–254.5 and 247.0–289.4, respectively. For the commercial cleaning procedure, the membrane flux at the beginning of the third cycle was 210.6, which was lower than the flux after the second cycle (240.9) and indicated a slightly negative flux recovery. The membrane flux varied from 218.2 to 203.0 during the third cycle and declined to 203.0 at the end of the filtration. However, after cleaning the membrane using our innovative cleaning procedures, the membrane flux was restored to 298.5, which showed a significant flux recovery. Using the innovative cleaning procedures, the membrane flux decreased from 298.5 to 247.0, increased to 372.7 and decrease to 283.3, and finally, increased to 356.1 and decreased to 289.4 for the first, second and third filtration cycles, respectively. These results demonstrated both the efficiency and stability of the innovative cleaning procedures. Furthermore, the permeation still met the requirements for oilfield injection or drainage without changes in the quality indexes (see Table S3), which indicated that the innovative cleaning procedures could provide preferable operational aspects during the UF process for polymer-flooding wastewater treatment. These results are promising for controlling membrane fouling cause by polymer-flooding wastewater.

4. Conclusions

Based on the flux recoveries and the FTIR and AFM force curve data, the molecular mechanisms of the individual cleaning reagents for the UF membranes in polymer-flooding wastewater treatment were as follows. (1) NaClO caused N–chlorination and C–N hydrolysis on the APAM amide groups and destroyed the hydrogen-bonded and interpenetrating polymer networks of the APAM fouling layer. (2) EDTA destroyed the coordination bonds of APAM–Ca and broke the egg-box shaped gel network. (3) DTAC micelles, not the monomers, enhanced the APAM–APAM intermolecular repulsions and destroyed the interpenetrating polymer network.

The combination of two of the abovementioned reagents showed a strong synergistic effect in both our sequential cleaning procedures and mixed solutions. Among them, the NaClO and DTAC solution (D + O) had the highest flux recovery (121%) in the bench-scale UF experiments. In the pilot-scale experiments, the tested innovative cleaning procedures (with formulated solutions of EDTA, NaClO and surfactants) promoted a flux recovery increasing by ~ 66% and a membrane flux rising by 21–32% during the UF process in comparison with that of the quondam commercial cleaning procedures. These results are expected to provide a universal theoretical and experimental basis for the design of cleaning procedures and control of UF membrane fouling in oilfield wastewater treatment.

Acknowledgements

This research was financially supported by the National Natural Science Foundation of China (Nos. 51578390, U1632135, 51678726, 51278225), Science and Technology Development Projects of Shandong Province (2016GGB01157), Shanghai Pujiang Program (No. 14PJ1432400), Shandong Provincial Natural Science Foundation (ZR2013EEQ007, ZR2015EM021), and the Key Projects in the National Science & Technology Pillar Program during the Twelfth-Five-Year Plan Period (No. 2012BAF03B06). We appreciate to Guozhuang Tian and Deqiang Wang for helping us in “Section 3.4”.

Appendix A. Supplementary material

Supplementary data associated with this article can be found in the online version at http://dx.doi.org/10.1016/j.memsci.2017.08.062.

References

[1] S.B. Deng, G. Yu, Z.P. Jiang, R.Q. Zhang, Y.P. Ting, Destabilization of oil droplets in produced water from ASP flooding, Colloid Surf. A-Physicochem. Eng. Asp. 252 (2005) 113–119.
[2] M. Lu, X.F. Wei, Treatment of oilfield wastewater containing polymer by the batch activated sludge reactor combined with a zerovalent iron/EDTA/air system, Bioresour. Technol. 102 (2011) 2555–2562.
[3] G.C. Liu, S.L. Yu, H.J. Yang, J. Hu, Y. Zhang, B. He, L. Li, Z.Y. Liu, Molecular mechanisms of ultrafiltration membrane fouling in polymer-flooding wastewater treatment: role of ions in polymeric fouling, Environ. Sci. Technol. 50 (2016) 1393–1402.
[4] S.B. Deng, R.B. Bai, J.P. Chen, Z.P. Jiang, G. Yu, F.S. Zhou, Z.X. Chen, Produced water from polymer flooding process in crude oil extraction: characterization and treatment by a novel crossflow oil-water separator, Sep. Purif. Technol. 29 (2002) 207–216.
[5] F.R. Ahmadun, A. Pendashteh, L.C. Abdullah, D.R.A. Biak, S.S. Madaeni,

Z.Z. Abidin, Review of technologies for oil and gas produced water treatment, J. Hazard. Mater. 170 (2009) 530–551.
[6] X.S. Yi, W.X. Shi, S.L. Yu, C. Ma, N. Sun, S. Wang, L.M. Jin, L.P. Sun, Optimization of complex conditions by response surface methodology for APAM-oil/water emulsion removal from aqua solutions using nano-sized TiO2/Al2O3 PVDF ultrafiltration membrane, J. Hazard. Mater. 193 (2011) 37–44.
[7] X.Y. Wang, Z. Wang, Y.N. Zhou, X.J. Xi, W.J. Li, L.Y. Yang, X.Y. Wang, Study of the contribution of the main pollutants in the oilfield polymer-flooding wastewater to the critical flux, Desalination 273 (2011) 375–385.
[8] B. Zhang, W.X. Shi, S.L. Yu, Y.B. Zhu, R.J. Zhanga, L. Li, Optimization of cleaning conditions on a polytetrafluoroethylene (PTFE) microfiltration membrane used in treatment of oil-field wastewater, RSC Adv. 5 (2015) 104960–104971.
[9] P. Sikorski, F. Mo, G. Skjak-Braek, B.T. Stokke, Evidence for egg-box-compatible interactions in calcium-alginate gels from fiber X-ray diffraction, Biomacromolecules 8 (2007) 2098–2103.
[10] G.D. Kang, C.J. Gao, W.D. Chen, X.M. Jie, Y.M. Cao, Q. Yuan, Study on hypochlorite degradation of aromatic polyamide reverse osmosis membrane, J. Membr. Sci. 300 (2007) 165–171.
[11] V.T. Do, C.Y.Y. Tang, M. Reinhard, J.O. Leckie, Degradation of polyamide nanofiltration and reverse osmosis membranes by hypochlorite, Environ. Sci. Technol. 46 (2012) 852–859.
[12] M. Nowakowska, K. Szczubialka, M. Grebosz, Interactions of temperature-responsive anionic polyelectrolytes with a cationic surfactant, J. Colloid Interface Sci. 265 (2003) 214–219.
[13] C.G. Bell, C.J.W. Breward, P.D. Howell, J. Penfold, R.K. Thomas, A theoretical analysis of the surface tension profiles of strongly interacting polymer-surfactant systems, J. Colloid Interface Sci. 350 (2010) 486–493.
[14] Q.L. Li, M. Elimelech, Organic fouling and chemical cleaning of nanofiltration membranes: measurements and mechanisms, Environ. Sci. Technol. 38 (2004) 4683–4693.
[15] X. Jin, X.F. Huang, E.M.V. Hoek, Role of specific ion interactions in seawater RO membrane fouling by alginic acid, Environ. Sci. Technol. 43 (2009) 3580–3587.
[16] T. Hugel, M. Seitz, The study of molecular interactions by AFM force spectroscopy, Macromol. Rapid Commun. 22 (2001) 989–1016.
[17] P. Hinterdorfer, Y.F. Dufrene, Detection and localization of single molecular recognition events using atomic force microscopy, Nat. Methods 3 (2006) 347–355.
[18] D.S. Zhao, S.L. Yu, A review of recent advance in fouling mitigation of NF/RO membranes in water treatment: pretreatment, membrane modification, and chemical cleaning, Desalin. Water Treat. 55 (2015) 870–891.
[19] S.T. Poele, J. van der Graaf, Enzymatic cleaning in ultrafiltration of wastewater treatment plant effluent, Desalination 179 (2005) 73–81.
[20] H. Yamamura, K. Kimura, Y. Watanabe, Mechanism involved in the evolution of physically irreversible fouling in microfiltration and ultrafiltration membranes used for drinking water treatment, Environ. Sci. Technol. 41 (2007) 6789–6794.
[21] I. Levitsky, A. Duek, R. Naim, E. Arkhangelsky, V. Gitis, Cleaning UF membranes with simple and formulated solutions, Chem. Eng. Sci. 69 (2012) 679–683.
[22] M.S. Manna, P. Saha, A.K. Ghoshal, Studies on the stability of a supported liquid membrane and its cleaning protocol, RSC Adv. 5 (2015) 71999–72008.
[23] R.R. Navarro, T. Hori, T. Inaba, K. Matsuo, H. Habe, A. Ogata, High-resolution phylogenetic analysis of residual bacterial species of fouled membranes after NaOCl cleaning, Water Res. 94 (2016) 166–175.
[24] W.W. Cai, Y. Liu, Enhanced membrane biofouling potential by on-line chemical cleaning in membrane bioreactor, J. Membr. Sci. 511 (2016) 84–91.
[25] X.M. Han, Z.W. Wang, X.Y. Wang, X. Zheng, J.X. Ma, Z.C. Wu, Microbial responses to membrane cleaning using sodium hypochlorite in membrane bioreactors: cell integrity, key enzymes and intracellular reactive oxygen species, Water Res. 88 (2016) 293–300.
[26] A. Piasecka, R. Bernstein, F. Ollevier, F. Meersman, C. Souffreau, R.M. Bilad, K. Cottenie, L. Vanysacker, C. Denis, I. Vankelecom, Study of biofilms on PVDF membranes after chemical cleaning by sodium hypochlorite, Sep. Purif. Technol. 141 (2015) 314–321.
[27] Y.C. Woo, J.J. Lee, L.D. Tijing, H.K. Shon, M.W. Yao, H.S. Kim, Characteristics of membrane fouling by consecutive chemical cleaning in pressurized ultrafiltration as pre-treatment of seawater desalination, Desalination 369 (2015) 51–61.
[28] Z.H. Zhang, M.W. Bligh, Y. Wang, G.L. Leslie, H. Bustamante, T.D. Waite, Cleaning strategies for iron-fouled membranes from submerged membrane bioreactor treatment of wastewaters, J. Membr. Sci. 475 (2015) 9–21.
[29] H.M. Ruan, Z.R. Yang, J.Y. Lin, J.N. Shen, J.B. Ji, C.J. Gao, B. Van der Bruggen, Biogas slurry concentration hybrid membrane process: pilot-testing and RO membrane cleaning, Desalination 368 (2015) 171–180.
[30] R.J. Zhang, S.L. Yu, W.X. Shi, J.Y. Tian, L.M. Jin, B. Zhang, L. Li, Z.Q. Zhang, Optimization of a membrane cleaning strategy for advanced treatment of polymer flooding produced water by nanofiltration, RSC Adv. 6 (2016) 28844–28853.
[31] P.L. Chen, Z.X. Zhong, F. Liu, W.H. Xing, Cleaning ceramic membranes used in treating desizing wastewater with a complex-surfactant SDBS-assisted method, Desalination 365 (2015) 25–35.
[32] L. Cui, P.Y. Chen, B.F. Zhang, D.Y. Zhang, J.Y. Li, F.L. Martin, K.S. Zhang, Interrogating chemical variation via layer-by-layer SERS during biofouling and cleaning of nanofiltration membranes with further investigations into cleaning efficiency, Water Res. 87 (2015) 282–291.
[33] C.H. Yu, L.C. Fang, S.K. Lateef, C.H. Wu, C.F. Lin, Enzymatic treatment for controlling irreversible membrane fouling in cross-flow humic acid-fed ultrafiltration, J. Hazard. Mater. 177 (2010) 1153–1158.
[34] J. Jung, Y.H. Ko, J.S. Choi, S. Lee, Optimization of chemical cleaning condition for microfiltration process using response surface methodology, Desalin. Water Treat. 57 (2016) 7466–7478.
[35] R. Bogati, C. Goodwin, K. Marshall, K.T. Leung, B.Q. Liao, Optimization of chemical cleaning for improvement of membrane performance and fouling control in drinking water treatment, Sep. Sci. Technol. 50 (2015) 1835–1845.
[36] O. Ferrer, B. Lefevre, G. Prats, X. Bernat, O. Gibert, M. Paraira, Reversibility of fouling on ultrafiltration membrane by backwashing and chemical cleaning: differences in organic fractions behaviour, Desalin. Water Treat. 57 (2016) 8593–8607.
[37] Y.S. Li, L. Yan, C.B. Xiang, L.J. Hong, Treatment of oily wastewater by organic-inorganic composite tubular ultrafiltration (UF) membranes, Desalination 196 (2006) 76–83.
[38] R. Oviedo-Roa, J.M. Martinez-Magadan, A. Munoz-Colunga, R. Gomez-Balderas, M. Pons-Jimenez, L.S. Zamudio-Rivera, Critical micelle concentration of an ammonium salt through DPD simulations using COSMO-RS-based interaction parameters, AIChE J. 59 (2013) 4413–4423.
[39] S. Miyagishi, H. Kurimoto, Y. Ishihara, T. Asakawa, Determination of the critical micelle concentrations and microviscosity with a fluorescence probe, auramine, Bull. Chem. Soc. Jpn. 67 (1994) 2398–2402.
[40] S.K. Mehta, K.K. Bhasin, R. Chauhan, S. Dham, Effect of temperature on critical micelle concentration and thermodynamic behavior of dodecyldimethylethylammonium bromide and dodecyltrimethylammonium chloride in aqueous media, Colloid Surf. A-Physicochem. Eng. Asp. 255 (2005) 153–157.
[41] J.J.H. Haftka, P. Scherpenisse, G. Oetter, G. Hodges, C.V. Eadsforth, M. Kotthoff, J.L.M. Hermens, Critical micelle concentration values for different surfactants measured with solid-phase microextraction fibers, Environ. Toxicol. Chem. 35 (2016) 2173–2181.
[42] C.L. Zhang, K.T. Valsaraj, W.D. Constant, D. Roy, Aerobic biodegradation kinetics of four anionic and nonionic surfactants at sub- and supra-critical micelle concentrations (CMCs), Water Res. 33 (1999) 115–124.
[43] S. Chauhan, K. Sharma, Effect of temperature and additives on the critical micelle concentration and thermodynamics of micelle formation of sodium dodecyl benzene sulfonate and dodecyltrimethylammonium bromide in aqueous solution: a conductometric study, J. Chem. Thermodyn. 71 (2014) 205–211.
[44] M. Kopycinska-Muller, R.H. Geiss, D.C. Hurley, Contact mechanics and tip shape in AFM-based nanomechanical measurements, Ultramicroscopy 106 (2006) 466–474.
[45] A.A. Thyparambil, Y. Wei, R.A. Latour, Determination of peptide-surface adsorption free energy for material surfaces not conducive to SPR or QCM using AFM, Langmuir 28 (2012) 5687–5694.
[46] R.G. Chaudhuri, S. Sunayana, S. Paria, Wettability of a PTFE surface by cationic-non-ionic surfactant mixtures in the presence of electrolytes, Soft Matter 8 (2012) 5429–5433.
[47] Z.H. Zhou, Q. Zhang, H.Z. Wang, Z.C. Xu, L. Zhang, D.D. Liu, L. Zhang, Wettability of a PTFE surface by aqueous solutions of zwitterionic surfactants: effect of molecular structure, Colloid Surf. A-Physicochem. Eng. Asp. 489 (2016) 370–377.
[48] P.-Gd Gennes, Scaling Concepts in Polymer Physics, Cornell University Press, Ithaca, New York, 1979.
[49] G.S. He, J. Yang, X.D. Zheng, Q. Wu, L.H. Guo, M.Q. Zhang, X.D. Chen, Entanglement and phase separation in hyperbranched polymer/linear polymer/solvent ternary blends, Polym. Test. 31 (2012) 182–190.
[50] C. Ray, J.R. Brown, A. Kirkpatrick, B.B. Akhremitchev, Pairwise interactions between linear alkanes in water measured by AFM force spectroscopy, J. Am. Chem. Soc. 130 (2008) 10008–10018.
[51] A. Noy, Force spectroscopy 101: how to design, perform, and analyze an AFM-based single molecule force spectroscopy experiment, Curr. Opin. Chem. Biol. 15 (2011) 710–718.
[52] C.J.V. Oss, Interfacial Forces in Aqueous Media, Marcel Dekker, NY, New York, 1994.
[53] P. Wang, Z.W. Wang, Z.C. Wu, Q. Zhou, D.H. Yang, Effect of hypochlorite cleaning on the physiochemical characteristics of polyvinylidene fluoride membranes, Chem. Eng. J. 162 (2010) 1050–1056.